Original Article

Docetaxel population pharmacokinetic modelling and simulation in Chinese cancer patients

Jian Wei[1], Yuwen Zhang[2], Ze Li[2], Xingang Li[2], Chenglong Zhao[3]

[1]Department of Interventional Radiography, Beijing Friendship Hospital, Capital Medical University, Beijing, China; [2]Department of Pharmacy, Beijing Friendship Hospital, Capital Medical University, Beijing, China; [3]Department of Pharmacy, Henan Provincial People's Hospital, People's Hospital of Zhengzhou University, Zhengzhou, China

Contributions: (I) Conception and design: X Li, C Zhao, J Wei; (II) Administrative support: J Wei; (III) Provision of study materials or patients: C Zhao; (IV) Collection and assembly of data: C Zhao; (V) Data analysis and interpretation: J Wei, X Li; (VI) Manuscript writing: All authors; (VII) Final approval of manuscript: All authors.

Correspondence to: Xingang Li. Department of Pharmacy, Beijing Friendship Hospital, Capital Medical University, 95 Yongan Road, Xicheng District, Beijing 100050, China. Email: lxg198320022003@163.com; Chenglong Zhao. Department of Pharmacy, Henan Provincial People's Hospital, 7 Weiwu, Zhengzhou 450003, China. Email: zhaocl725@zzu.edu.cn.

Background: Docetaxel is a widely prescribed cytotoxic chemotherapy drug for various cancers and the main dose-limiting toxicity is dose-dependent neutropenia. In China, the current dose regimen for docetaxel frequently results in high inter-individual pharmacokinetic (PK) variability. There is a very urgent need to establish a population PK model of docetaxel for Chinese cancer patients, to predict the area under the curve (AUC) based on the PK model and avoid toxicity, providing optimal drug dose guidance to clinicians.

Methods: Docetaxel was administered at a dose of 75 mg/m^2 once every 3 weeks, and at the scheduled time, blood samples were collected to measure the docetaxel concentration. A nonlinear, mixed-effects modelling approach was used to fit the plasma concentration-time data. A two-compartmental model was selected to characterize the *in vivo* behavior of docetaxel. Using population modelling, various covariates were explored to ascertain their impact on the docetaxel PK. Monte Carlo simulations were performed to derive the optimal individualized dose regimen.

Results: A total of 440 patients with 880 concentration data were collected. The covariate selection indicated that age, body mass index (BMI), and body surface area (BSA) had significant correlations with docetaxel clearance (CL). Bootstrap and visual predictive check (VPC) indicated that a robust and reliable PK model had been established. The final population model was effectively used for simulation to determine docetaxel dose regimens for Chinese cancer patients. Aiming an AUC <2.6 mg/L·h, a simple to use dose regimen was derived based on Monte Carlo simulations.

Conclusions: A population PK model of docetaxel for Chinese cancer patients was developed and validated, showing that age, BMI, and BSA were significantly associated with CL. A simple to use dose regimen table was created to guide clinicians.

Keywords: Docetaxel; population pharmacokinetics; age; body mass index (BMI); body surface area (BSA)

Submitted Apr 28, 2022. Accepted for publication Jun 20, 2022.
doi: 10.21037/atm-22-2619
View this article at: https://dx.doi.org/10.21037/atm-22-2619

Introduction

Docetaxel, a widely prescribed cell-cycle specific cytotoxic chemotherapy drug for various cancers, can promote tubules to assemble into stable microtubules and inhibit their depolymerizations, eventually resulting in cell death to prevent tumor growth (1,2). As we know, the appropriate dose of chemotherapeutic drugs is a key point for anticancer therapy. Overdose of drugs may lead

© Annals of Translational Medicine. All rights reserved.

to severe hematological toxicity and result in treatment failure (2-4). The main dose-limiting toxicity of docetaxel is neutropenia, which is a dose-dependent, reversible, and noncumulative leukoneutropenia (5,6). Currently, in clinical practice, the dose of docetaxel is determined by the patient's body surface area (BSA) and is recommended at 75 mg/m^2 (2,7,8). However, the drug-blood concentration of docetaxel between different patients has shown great inter-individual variability (IIV) (9). Research has revealed that there are factors other than the BSA that affect the pharmacokinetics (PK) of docetaxel, such as liver function, age, weight, and albumin (ALB), co-administration of ritonavir which may be related to the docetaxel clearance (CL) (10-16). Nonetheless, there have been few reports about the other factors, and to date, no model based on Chinese cancer patients has been developed. In China, the dose of docetaxel is strictly prescribed according to the patient's BSA, and it requires therapeutic drug monitoring (TDM) due to the great IIV. At the same time, numerous studies have shown that the area under the curve (AUC) of docetaxel is an independent predictor of drug toxicity (17,18). As a result, it is necessary to establish docetaxel population PK model for Chinese cancer patients, to predict the AUC and avoid toxicity. We aimed to explore the factors that influence the PK of docetaxel in Chinese cancer patients and provide information for the individualization of docetaxel dose. We present the following article in accordance with the MDAR reporting checklist (available at https://atm.amegroups.com/article/view/10.21037/atm-22-2619/rc).

Methods

Patient selection

This study was conducted in Henan Provincial People's Hospital. The inclusion criteria were as follows: (I) patients were diagnosed with cancer; and (II) patients were treated with docetaxel. Patients were excluded if any of the following conditions applied: pregnant (19) or nursing women; previously received docetaxel chemotherapy; severe hypertension, diabetes or clinically significant complications; or combined with radiotherapy and other anticancer therapy. The baseline characteristics of the enrolled patients included: gender, age, body weight (BW), body mass index (BMI), ALB, BSA, hemoglobin (HGB), platelet (PLT), total protein (TP), leukocyte [white blood cell (WBC)], alanine aminotransferase (ALT), aspartate aminotransferase (AST), alkaline phosphatase (ALP), lactate dehydrogenase (LDH), total bilirubin (TBIL), and creatinine (CREA). These data were retrieved from the patient's medical record.

Study design

All participants received docetaxel by intravenous infusion. According to the dose guideline of docetaxel on the drug label, docetaxel was administered at a dose of 75 mg/m^2 once every 3 weeks. Docetaxel was diluted with 250 mL of 0.9% sodium chloride injection or 5% glucose injection as a solvent and infused within 2 hours. Two blood samples were collected from each participant: (I) during the intravenous drip, 2 mL of peripheral venous blood was collected as monitoring blood sample I; (II) after the drip, 2 mL of peripheral venous blood was collected as monitoring blood sample II. The samples were separated by centrifugation at 3,000 r/min for 10 minutes (4 ℃), and the separated plasmas were then suctioned and preserved at −80 ℃ until analysis. The plasma concentrations were detected by Dirui CS-600 auto-chemistry biochemical analyzer (Changchun, China) and MyDocetaxel kit (Pennsylvania, USA) (20).

The study was conducted in accordance with the Declaration of Helsinki (as revised in 2013). The study was approved by institutional ethics committee of Henan Provincial People's Hospital [2020 (Ethical Review) No. 11]. Written informed consent was obtained from patients or their parental/legal guardians. This study was not applicable to clinical trial registration because the participants received standard treatment.

Structural model development

Simple compartmental models were used to describe the docetaxel PK. A nonlinear mixed-effects modelling (NONMEM) approach was applied to develop the PK model using the Phoenix® NLME™ 7.0 (Certara, St. Louis, MO, USA) software, with first-order conditional estimation and extended least squares (FOCE-ELS) method. All PK parameters accorded with a log-normal distribution.

$$P_i = P \times e^{\eta i} \quad [1]$$

P and Pi represent the typical value of a PK parameter and the ith patient's individual parameter, respectively. The random variable η_i is normally distributed with a mean of zero and a variance of ω^2. The residual error is characterized by the proportional error model (Eq. [1]).

$$C_i = C \times (1+\varepsilon) \quad [2]$$

C_i and C represent the individual plasma concentration

© Annals of Translational Medicine. All rights reserved.

and predictions of plasma concentrations, respectively. ε accounts for the proportional errors of predictions for drug concentrations, which are normally distributed with a mean of zero and a variance of σ^2 (Eq. [2]).

Population model

Covariate analyses were undertaken to evaluate the impact of docetaxel PK. The covariates in dataset were divided into two categories: continuous covariates and categorical covariates. Continuous covariates include age, BW, BMI, BSA, AST, ALT, TBIL, CREA CL (determined by the Cockcroft-Gault formula) and the categorical covariate was gender. A proportional shift function was used to assess the effect of the categorical covariate on each parameter. Continuous covariates were centered at their median values, and linear, exponential, and power functions were used to assess the effect of each covariate on the PK parameters (Eq. [3]).

$$P_i = P \times \left(\frac{Cov}{Cov_{median}} \right)^{\theta} \times e^{\eta i} \quad [3]$$

The forward inclusion followed by the backward elimination method was applied to establish the final PK model. A covariate was considered significant when the addition resulted in a decrease of the objective function value (OFV) >6.635 (P<0.01) and the elimination resulted in an increase of the OFV >10.828 (P<0.001).

Model evaluation and validation

The reliability of the base structural model and the final model was assessed visually by using goodness-of-fit plots and observing the trend in the plots. Four scatter plots were contained in goodness-of-fit plots: conditional weighted residuals (CWRES) versus time after dose, CWRES versus population predictions (PRED), observations versus PRED, and CWRES versus standard normal quantiles. The prediction performance and stability of the final model were evaluated by visual predictive checks (VPCs) and bootstrap resampling method (21,22). After random sampling, 2,000 new datasets with different patient combinations were generated and parameters were re-estimated after using the final population model. We then compared the median parameter value and its 95% confidence intervals (CIs) with the estimate from the final model. In addition, 2,000 virtual datasets were simulated based on the final population model to compare the distribution characteristics of the predicted values with the measured values. The observations were displayed overlaid on the simulated 5th percentiles, median, and 95th percentiles.

Simulation

The main purpose of the simulations was to offer dose counsels for the clinical administration of docetaxel to Chinese cancer patients. In consideration of the plasma representing the effect site, Monte Carlo simulations (2,000 patients) were performed to create the plasma drug concentrations-time data. Non-compartment analysis was used to calculate the AUC of simulation data. An AUC <2.6 mg/L·h is the pharmacokinetic/pharmacodynamic (PK/PD) target attainment associated with the toxicity (23). The plasma-drug concentration date was calculated at different times utilizing the relationship between covariates and PK parameters in final population PK model. To perform the deterministic simulations, we fixed the typical values to the final parameter estimates and fixed IIV to 0. Patients were divided into subgroups based on covariates significantly associated with PK. In order to figure out the optimal individualized dose regimens for patients from different subgroups, simulations were performed using Phoenix NLME software. Based on the simulation results, we derived an easy-to-use dose regimen table.

Results

Baseline information

In accordance with the inclusion criteria, a total of 440 patients (17 males and 423 females) were enrolled in this study, and 880 plasma concentration data were collected. The demographic and clinical characteristics of the enrolled patients are summarized in *Table 1*.

Population PK model

A two-compartment model was used to characterize the PK of docetaxel. After forward inclusion and backward elimination of all covariates, age, BMI and BSA were identified and included in the final population PK model. Their relationships in the final model were described as follows:

$$CL_i = 38.20 \times \left(\frac{BMI}{24.84} \right)^{1.31} \times \left(\frac{BSA}{1.61} \right)^{0.99} \times \left(\frac{AGE}{50} \right)^{-0.72} \times e^{\eta i} \left(L/h \right) \quad [4]$$

© Annals of Translational Medicine. All rights reserved.

Table 1 Demographic and clinical characteristics of enrolled patients for modelling (n=440)

Variables	Median	Range	Average	SD
Dosage (μg)	120,000	60,000 to 200,000	126,493	24,377
Duration (h)	1.00	0.83 to 4.00	1.13	0.32
Age (years)	50	13 to 79	50	10
BW (kg)	62	43 to 97	63	9
BMI (kg/m^2)	24.84	17.18 to 36.31	24.91	3.58
ALB (g/L)	39.2	25.8 to 49.6	38.75	4.2
BSA (m^2)	1.61	1.29 to 2.15	1.62	0.13
HGB (g/L)	111	74 to 224	111	15
PLT (×10^9/L)	246	48 to 565	255	86
TP (g/L)	67.6	51.2 to 82.9	67.5	6.4
WBC (×10^9/L)	5.98	2.28 to 52.69	7.76	6.08
ALT (U/L)	20	6 to 187	28	22
AST (U/L)	21	9 to 131	27	17
ALP (U/L)	69.0	6.4 to 242.0	73.1	25.3
LDH (U/L)	214	83 to 2,011	226	124
TBIL (μmol/L)	7.3	2.8 to 29.0	8.0	3.5
CREA (μmol/L)	46.00	3.45 to 151.00	47.93	12.99

BW, body weight; BMI, body mass index; ALB, albumin; BSA, body surface area; HGB, hemoglobin; PLT, platelet; TP, total protein; WBC, white blood cell; ALT, alanine aminotransferase; AST, aspartate aminotransferase; ALP, alkaline phosphatase; LDH, lactate dehydrogenase; TBIL, total bilirubin; CREA, creatinine; SD, standard deviation.

$$V_{ci}=5.73\times e^{\eta i}\left(L\right) \quad [5]$$

$$Q_i=40.99\times e^{\eta i}\left(L/h\right) \quad [6]$$

$$V_{pi}=270.87\times e^{\eta i}\left(L\right) \quad [7]$$

In Eq. [4], 38.20 L/h was the typical value of docetaxel CL; 1.31 and 0.99 represented the estimated coefficient describing the associations between BMI and CL, BSA and CL, with CL increasing when BMI and BSA ascended; and −0.72 indicated the estimated coefficient describing the relationship between the age and CL, with CL decreasing when the age increased. In Eqs. [5-7], 24.84, 1.61 and 50 were median values of BMI, BSA and age, respectively. The typical values of V_c, Q and V_p were 5.73 L, 40.99 L/h and 270.87 L, respectively. All parameters were estimated with an acceptable accuracy [relative standard error (RSE) ranged from 2.55% to 5.45%]. *Table 2* indicates the parameter estimates of the final population PK model.

Goodness-of-fit and model validation

Between the base model and final model, the scatter plots among observations and PRED were compared with each other (*Figure 1A-1D*). We applied CWRES versus time, PRED, and standard normal quantiles to test if any misspecifications existed in base and final models (*Figure 1E-1F*). In the base model, an association of the parameters' ETAS (inter-individual variations) (CL) and covariates (age, BMI, and BSA) could be observed (*Figure 2*), so the three covariates were added to parameter CL in the final model. After the incorporation of age, BMI, and BSA, the above association disappeared, suggesting a significant improvement in the final model (*Figure 2*). In these plots, there was no obvious systematic bias observed, and the proposed final model was able to describe docetaxel PK in enrolled patients appropriately. Plots of correlation between PK parameters and all covariates in the base and final models are displayed in Figure S1.

The median values were roughly the same as the original

© Annals of Translational Medicine. All rights reserved.

Table 2 Parameter estimates and bootstrap results of the final population pharmacokinetic model

Parameter (unit)	Model estimates				Bootstrap results		
	Estimate	RSE%	95% CI	IIV (CV%)	Median	95% CI	IIV (CV%)
CL (L/h)	38.20	4.54	34.80 to 41.60	52.42	37.99	29.53 to 44.44	53.40
V_c (L)	5.73	5.41	5.13 to 6.34	48.00	5.75	4.20 to 6.41	48.21
Q (L/h)	40.99	2.55	38.94 to 43.04	0.32	41.83	35.76 to 47.70	0.42
V_p (L)	270.87	5.45	241.8 to 299.85	0.05	268.15	199.13 to 344.00	0.06
f_{Age-CL}	–0.72	4.81	–0.79 to –0.65	NA	–0.71	–0.82 to –0.51	NA
f_{BMI-CL}	1.31	4.84	1.19 to 1.43	NA	1.35	1.18 to 1.53	NA
f_{BSA-CL}	0.99	2.72	0.93 to 1.04	NA	1.04	0.72 to 1.23	NA
Residual error (proportional error, CV%)							
σ	27.28	4.28	24.99 to 29.57	NA	26.90	25.69 to 28.96	NA

CL, docetaxel clearance; Q, inter-compartment clearance; V_c, distribution volume of central compartment; V_p, distribution volume of the peripheral compartment; f, coefficient; BMI, body mass index; BSA, body surface area; RSE, relative standard error; CI, confidence interval; IIV, inter-individual variability; CV, coefficient variation; IIV, inter-individual variability; NA, not available.

parameter estimates, and the values estimated during data fitting were contained in the 95% CIs. Bootstrapping showed acceptable robustness of the final population PK model. *Table 2* listed the bootstrap results which included the median parameter estimate with 95% CI. Docetaxel VPCs plots visually displayed the actual observed values and 5th to 95th percentiles, or in other words, the 90% prediction intervals (PI). The plots showed the 5th and 95th percentiles (dashed lines) and the 50th percentiles (solid lines). From this plot, we can see that most observations fall within the 90% PI, which indicated the sufficient predictive properties of the final population model (*Figure 3*).

Simulation

Three covariates (age, BMI, and BSA) were included in the final model, patients were categorized by age (<40, 40–60, >60 years), BMI (<18, 18–24, >24 kg/m^2), and BSA (<1.4, 1.4–1.59, 1.6–1.8, >1.8 m^2). To prevent results distortion, we limited the ranges of covariates in simulation to the observed ranges in the modeled data. Other parameters values were fixed to the population typical values and random variability was fixed to zero. The simulations were performed to create ten simulated concentrations-time for each patient. The AUC was calculated using the trapezoid method. With the goal of an AUC <2.6 mg/L·h, the optimal doses for different subgroups of patients were derived. To evaluate the recommended dose regimens we derived, we applied Monte Carlo simulations with 2,000 simulated patients (IIV implemented) and the percent probabilities of PK/PD target attainment (AUC <2.6 mg/L·h) associated with age, BMI, and BSA values were determined. The dose regimens showing the percent probabilities of PK/PD target attainment of at least 80% are shown in *Table 3*. The results of this simulation only apply to patients whose age, BMI, and BSA were within the ranges observed in the modeled data. Simulation results illustrated that the recommended dose needed to be decreased as the age increased to maintain optimal exposures, while the recommended dose needed to be increased as BMI and BSA ascended.

Discussion

Neutropenia is the main dose-limiting toxicity of docetaxel treatment. This toxicity may be life-threatening and often imposes a delay on subsequent administration that affects treatment efficacy (5). Previous studies (17,18,24-27) had revealed that the AUC of docetaxel was associated with neutropenia, and it was a predictor of the docetaxel toxicity. Consistent with most anticancer drugs, to date, docetaxel has been administered based on BSA in clinical practice (28). However, this ordinary method of calculating doses may not be appropriate for all patients due to the IIV. The drug concentrations of docetaxel for different patients might fluctuate in a large range (up to 11.45-fold) at the same time point (9). Docetaxel administration based on BSA cannot

© Annals of Translational Medicine. All rights reserved.

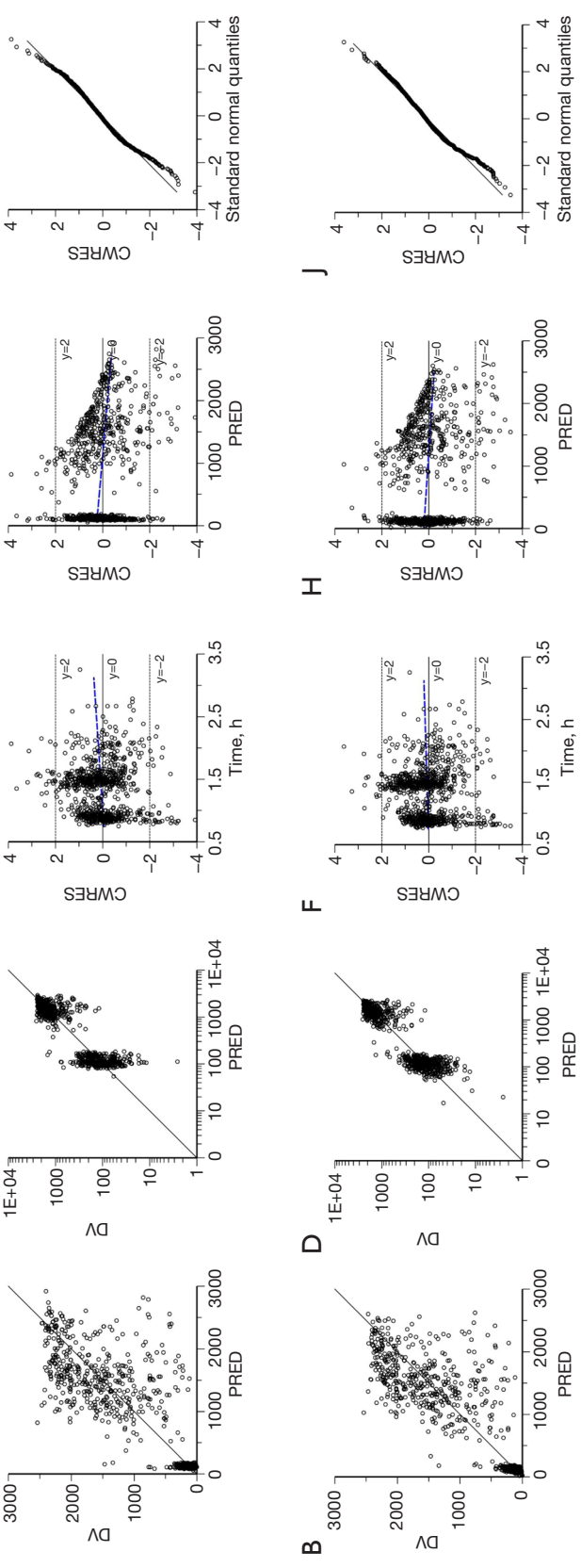

Figure 1 Goodness-of-fit plots of pharmacokinetic modelling for docetaxel. (A) Observations versus PRED in the base model and the line represents the unity of y = x; (B) observations versus PRED in the final mode and the line represents the unity of y = x; (C,D) the local amplification images of (A,B); (E) CWRES versus time in the base model; (F) CWRES versus time in the final model; (G) CWRES versus PRED in the base model; (H) CWRES versus PRED in the final model; (I) CWRES versus standard normal quantiles in the base model and the line represents the unity of y = x; (J) CWRES versus standard normal quantiles in the final model and the line represents the unity of y = x. DV, dependent value (observations); PRED, population predictions; CWRES, conditional weighted residuals.

© Annals of Translational Medicine. All rights reserved.

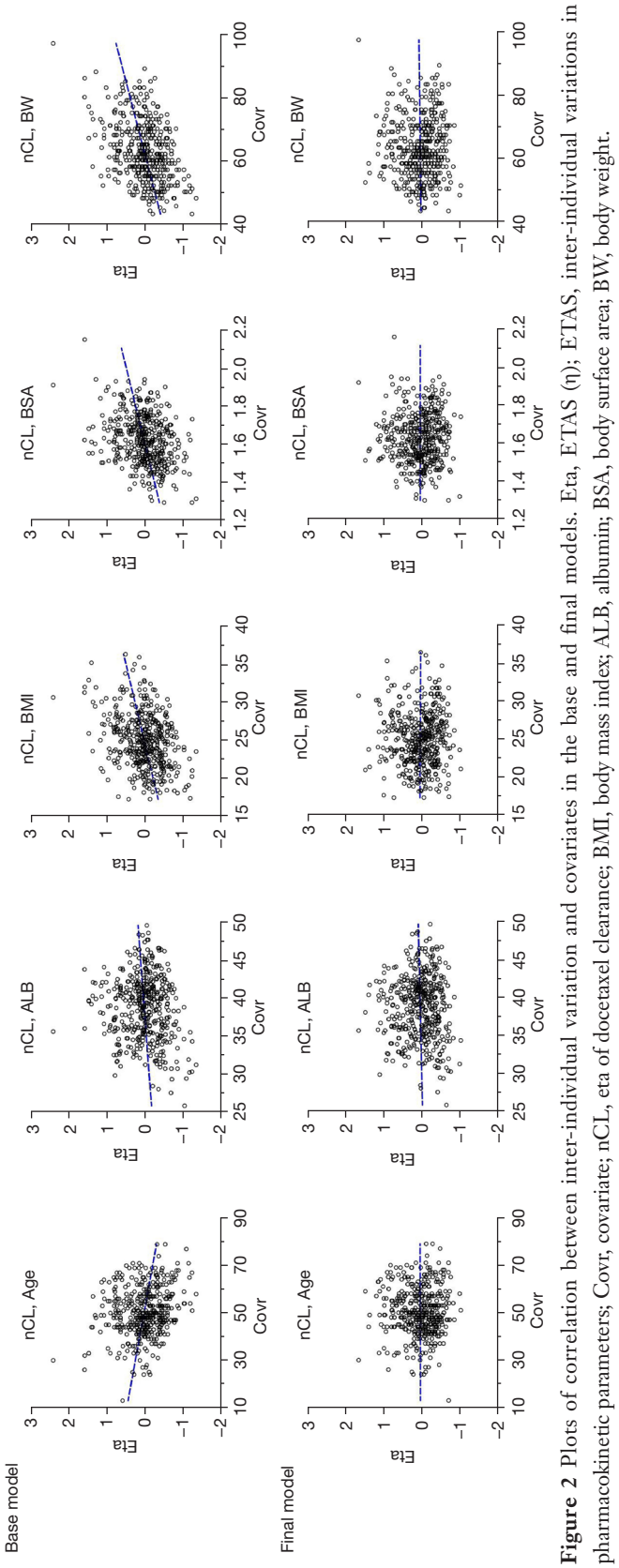

Figure 2 Plots of correlation between inter-individual variation and covariates in the base and final models. Eta, ETAS (η); ETAS, inter-individual variations in pharmacokinetic parameters; Covr, covariate; nCL, eta of docetaxel clearance; BMI, body mass index; ALB, albumin; BSA, body surface area; BW, body weight.

satisfactorily predict the blood-docetaxel concentration and avoid the toxicity for individuals. Until now, the optimal dose of docetaxel for Chinese cancer patients had not been investigated. We aimed to establish a population PK model of docetaxel for Chinese cancer patients to explore the other factors that influence the PK of docetaxel and provide information for individualization of docetaxel dose based on the PK/PD target attainment of AUC.

Our study involved 880 plasma-drug concentration data of 440 patients. We developed a population PK model of docetaxel in Chinese cancer patients by NONMEM, revealing that the age, BMI, and BSA of patients showed significant effects on the drug CL. This suggested that the age, BMI, and BSA of patients should be comprehensively considered in the clinical medication and might contribute to precision medication in the future. In addition, according to the PK/PD target attainment of an AUC <2.6 mg/L·h, a simple-to-use dose regimen table was derived based on Monte Carlo simulations (2,000 patients). As far as we know, this is the first report to evaluate the blood PK profile of docetaxel through population modelling and simulation in Chinese cancer patients. This is the biggest advantage of this model.

As proved by another study, a three-compartmental model best represented plasma docetaxel concentration-time data (14). At first, we attempted to develop a three-compartment model, while the parameters were very unstable and the OFV decline was not significant (P>0.05). We considered that the relatively sparse blood samples collected mostly during or after the drip made it difficult to develop a complex compartment model. In addition, we also developed a single-compartment model, from which a large system deviation and a significant underestimation of the elimination phase data were observed. Finally, based on the two-compartmental model, we found that the plasma concentrations fit and the predicted values supported the observations well. Significant relationships between age, BMI, BSA, and CL were observed in the final PK model, indicating that the two-compartmental model was valid.

The drug CL of docetaxel decreased significantly with the increase of age in the final model. This correlation may be attributed to CYP3A, which is the primary enzyme responsible for the metabolism of docetaxel. A previous study has shown age-related declines in the *in vitro* activities of CYP3A (29). In addition, it has been demonstrated that elderly patients are more prone to neutropenia due to the increasing docetaxel exposure (30). On the contrary, with the rise of BMI, CL increased significantly, which might be

© Annals of Translational Medicine. All rights reserved.

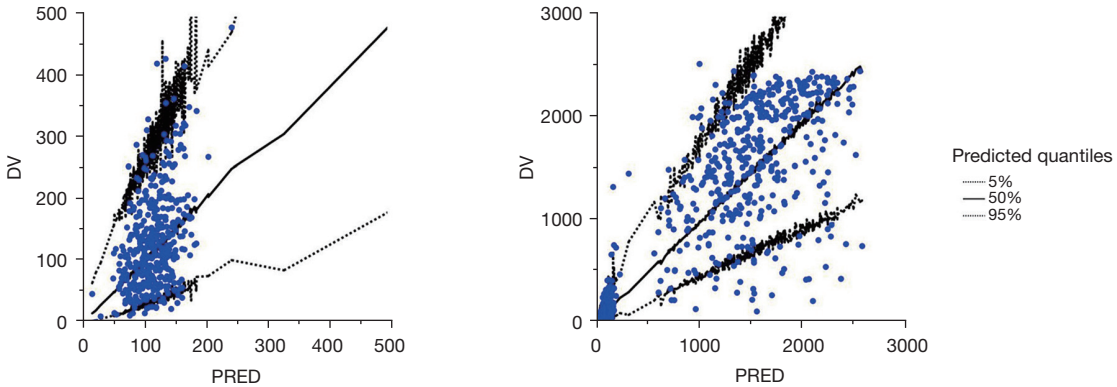

Figure 3 The visual predictive check plots (final population pharmacokinetic model). The actual original observations (blue dots). The 5% and 95% quantiles (black dashed lines) and the 50% quantiles (black solid lines) from the simulated observations. DV, dependent value (observations); PRED, population predictions.

Table 3 Docetaxel dose regimens for Chinese cancer patients based on age, BMI, and BSA (AUC <2.6 mg/L·h)

BMI, kg/m^2	Docetaxel dose (mg)		
	<40 years	40–60 years	>60 years
BSA <1.4 m^2			
<18	145	125	95
18–24	175	130	120
>24	190	165	140
BSA =1.4–1.59 m^2			
<18	150	140	110
18–24	190	145	125
>24	195	170	150
BSA =1.6–1.8 m^2			
<18	155	145	115
18–24	195	160	130
>24	200	175	170
BSA >1.8 m^2			
<18	160	150	130
18–24	200	180	150
>24	220	200	180

BMI, body mass index; BSA, body surface area; AUC, area under the curve.

explained by the lipophilic nature of docetaxel. The bulky polycyclic rings of docetaxel led to a high affinity for the adipose tissue and required metabolic transformation in the liver to eliminate. As the research reported, obesity induced changes in the hepatic CL of lipophilic drugs, whose sulfo-conjugation or glucurono-conjugation were increased (31). This may eventually result in an increase in CL for patients with a high BMI.

© Annals of Translational Medicine. All rights reserved.

Docetaxel is metabolized in the liver and eliminated mainly by the feces through the biliary tract, so drug CL is reduced in patients with abnormal liver function. In this study, the values of AST and ALT of 80.68% of patients were in the normal range, indicating most of the participants had a normal liver function. The proportion of patients with hepatic impairment was insufficient, so the final model was more suitable for patients with normal liver function. Docetaxel is a lipophilic drug with a high protein-binding rate. The α1-acid glycoprotein (AGP), an important component of serum ALB, is the main protein that binds to docetaxel, which is regarded a determinant for docetaxel PK (17,32). However, no effect of AGP on CL was observed in this study. This may be due to the decreasing of free fraction when AGP levels increase, whereby CL of unbound drugs may be only slightly affected by AGP levels (23).

Several limitations of this study should be noted: (I) most blood samples were recorded as having been collected during or after the drip at a given time, which might not have completely represented the real blood collection time in clinical practice, and this could have led to the distortion of the final model. A follow-up study with more accurate blood collection time is needed to confirm the study conclusions; (II) due to the sparse blood samples, the three-compartmental model developed by the previous study was not applied; and (III) patients with normal liver function were the main components in the final model, so the conclusion in this study is not transferrable to patients with abnormal liver function. This is the biggest disadvantage of this model.

Conclusions

We developed a docetaxel plasma population PK model in Chinese cancer patients. Age, BMI, and BSA were identified as significant covariates influencing the docetaxel plasma concentration. Simulations were performed based on the final PK model, and based on the results, we derived a simple-to-use dose regimen table. These study results may assist clinicians in the selection of an optimal docetaxel dose regimen for the treatment of Chinese cancer patients.

Acknowledgments

Funding: None.

Footnote

Reporting Checklist: The authors have completed the MDAR reporting checklist. Available at https://atm.amegroups.com/article/view/10.21037/atm-22-2619/rc

Data Sharing Statement: Available at https://atm.amegroups.com/article/view/10.21037/atm-22-2619/dss

Conflicts of Interest: All authors have completed the ICMJE uniform disclosure form (available at https://atm.amegroups.com/article/view/10.21037/atm-22-2619/coif). The authors have no conflicts of interest to declare.

Ethical Statement: The authors are accountable for all aspects of the work in ensuring that questions related to the accuracy or integrity of any part of the work are appropriately investigated and resolved. The study was conducted in accordance with the Declaration of Helsinki (as revised in 2013). The study was approved by institutional ethics committee of Henan Provincial People's Hospital [2020 (Ethical Review) No. 11]. Written informed consent was obtained from patients or their parental/legal guardians.

Open Access Statement: This is an Open Access article distributed in accordance with the Creative Commons Attribution-NonCommercial-NoDerivs 4.0 International License (CC BY-NC-ND 4.0), which permits the non-commercial replication and distribution of the article with the strict proviso that no changes or edits are made and the original work is properly cited (including links to both the formal publication through the relevant DOI and the license). See: https://creativecommons.org/licenses/by-nc-nd/4.0/.

References

1. Al-Batran SE, Homann N, Pauligk C, et al. Perioperative chemotherapy with fluorouracil plus leucovorin, oxaliplatin, and docetaxel versus fluorouracil or capecitabine plus cisplatin and epirubicin for locally advanced, resectable gastric or gastro-oesophageal junction adenocarcinoma (FLOT4): a randomised, phase 2/3 trial. Lancet 2019;393:1948-57.
2. Rosenthal SA, Hu C, Sartor O, et al. Effect of Chemotherapy With Docetaxel With Androgen Suppression and Radiotherapy for Localized High-Risk Prostate Cancer: The Randomized Phase III NRG Oncology RTOG 0521 Trial. J Clin Oncol 2019;37:1159-68.
3. Mei T, An X, Zhan J, et al. Docetaxel exposure and hematological toxicity in Chinese patients with locally

© Annals of Translational Medicine. All rights reserved.

advanced/metastatic nasopharyngeal carcinoma. Int J Clin Pharmacol Ther 2021;59:216-23.
4. Rosenberg AJ, Rademaker A, Hochster HS, et al. Docetaxel, Oxaliplatin, and 5-Fluorouracil (DOF) in Metastatic and Unresectable Gastric/Gastroesophageal Junction Adenocarcinoma: A Phase II Study with Long-Term Follow-Up. Oncologist 2019;24:1039-e642.
5. Puisset F, Alexandre J, Treluyer JM, et al. Clinical pharmacodynamic factors in docetaxel toxicity. Br J Cancer 2007;97:290-6.
6. Ma Y, Zhao X, Chen X, et al. Therapeutic drug monitoring of docetaxel by pharmacokinetics and pharmacogenetics: A randomized clinical trial of AUC-guided dosing in nonsmall cell lung cancer. Clin Transl Med 2021;11:e354.
7. Kenmotsu H, Tanigawara Y. Pharmacokinetics, dynamics and toxicity of docetaxel: Why the Japanese dose differs from the Western dose. Cancer Sci 2015;106:497-504.
8. Heineman T, Baumgart M, Nanavati C, et al. Safety and pharmacokinetics of docetaxel in combination with pegvorhyaluronidase alfa in patients with non-small cell lung cancer. Clin Transl Sci 2021;14:1875-85.
9. Rudek MA, Sparreboom A, Garrett-Mayer ES, et al. Factors affecting pharmacokinetic variability following doxorubicin and docetaxel-based therapy. Eur J Cancer 2004;40:1170-8.
10. Hurria A, Fleming MT, Baker SD, et al. Pharmacokinetics and toxicity of weekly docetaxel in older patients. Clin Cancer Res 2006;12:6100-5.
11. Nieuweboer AJ, de Morrée ES, de Graan AJ, et al. Inter-patient variability in docetaxel pharmacokinetics: A review. Cancer Treat Rev 2015;41:605-13.
12. Charles KA, Rivory LP, Stockler MR, et al. Predicting the toxicity of weekly docetaxel in advanced cancer. Clin Pharmacokinet 2006;45:611-22.
13. Patil A, Shriyan B, Mehta P, et al. ADME gene polymorphisms do not influence the pharmacokinetics of docetaxel: Results from a population pharmacokinetic study in Indian cancer patients. Cancer Med 2021;10:4948-56.
14. Minami H, Kawada K, Sasaki Y, et al. Population pharmacokinetics of docetaxel in patients with hepatic dysfunction treated in an oncology practice. Cancer Sci 2009;100:144-9.
15. Hooker AC, Ten Tije AJ, Carducci MA, et al. Population pharmacokinetic model for docetaxel in patients with varying degrees of liver function: incorporating cytochrome P4503A activity measurements. Clin Pharmacol Ther 2008;84:111-8.
16. Koolen SL, Oostendorp RL, Beijnen JH, et al. Population pharmacokinetics of intravenously and orally administered docetaxel with or without co-administration of ritonavir in patients with advanced cancer. Br J Clin Pharmacol 2010;69:465-74.
17. Bruno R, Olivares R, Berille J, et al. Alpha-1-acid glycoprotein as an independent predictor for treatment effects and a prognostic factor of survival in patients with non-small cell lung cancer treated with docetaxel. Clin Cancer Res 2003;9:1077-82.
18. Alexandre J, Rey E, Girre V, et al. Relationship between cytochrome 3A activity, inflammatory status and the risk of docetaxel-induced febrile neutropenia: a prospective study. Ann Oncol 2007;18:168-72.
19. Janssen JM, Van Calsteren K, Dorlo TPC, et al. Population Pharmacokinetics of Docetaxel, Paclitaxel, Doxorubicin and Epirubicin in Pregnant Women with Cancer: A Study from the International Network of Cancer, Infertility and Pregnancy (INCIP). Clin Pharmacokinet 2021;60:775-84.
20. Jia MM, Zhang J, Zuo LH, et al. Evaluation of latex-enhanced turbidimetric immunoassay for determining docetaxel concentrations and its clinical application. China Journal of Hospital Pharmacy 2016;36:2184-7.
21. Li X, Wu Y, Sun S, et al. Population Pharmacokinetics of Vancomycin in Postoperative Neurosurgical Patients and the Application in Dosing Recommendation. J Pharm Sci 2016;105:3425-31.
22. Li X, Wu Y, Sun S, et al. Population Pharmacokinetics of Vancomycin in Postoperative Neurosurgical Patients. J Pharm Sci 2015;104:3960-7.
23. Bruno R, Vivier N, Vergniol JC, et al. A population pharmacokinetic model for docetaxel (Taxotere): model building and validation. J Pharmacokinet Biopharm 1996;24:153-72.
24. Extra JM, Rousseau F, Bruno R, et al. Phase I and pharmacokinetic study of Taxotere (RP 56976; NSC 628503) given as a short intravenous infusion. Cancer Res 1993;53:1037-42.
25. Goh BC, Lee SC, Wang LZ, et al. Explaining interindividual variability of docetaxel pharmacokinetics and pharmacodynamics in Asians through phenotyping and genotyping strategies. J Clin Oncol 2002;20:3683-90.
26. Ozawa K, Minami H, Sato H. Logistic regression analysis for febrile neutropenia (FN) induced by docetaxel in Japanese cancer patients. Cancer Chemother Pharmacol 2008;62:551-7.
27. Minami H, Kawada K, Sasaki Y, et al. Pharmacokinetics and pharmacodynamics of protein-unbound docetaxel in

© Annals of Translational Medicine. All rights reserved.

cancer patients. Cancer Sci 2006;97:235-41.
28. Gurney H. Dose calculation of anticancer drugs: a review of the current practice and introduction of an alternative. J Clin Oncol 1996;14:2590-611.
29. Schmucker DL. Liver function and phase I drug metabolism in the elderly: a paradox. Drugs Aging 2001;18:837-51.
30. ten Tije AJ, Verweij J, Carducci MA, et al. Prospective evaluation of the pharmacokinetics and toxicity profile of docetaxel in the elderly. J Clin Oncol 2005;23:1070-7.
31. Cheymol G. Clinical pharmacokinetics of drugs in obesity. An update. Clin Pharmacokinet 1993;25:103-14.
32. Lombard A, Mistry H, Aarons L, et al. Dose individualisation in oncology using chemotherapy-induced neutropenia: Example of docetaxel in non-small cell lung cancer patients. Br J Clin Pharmacol 2021;87:2053-63.

(English Language Editor: J. Jones)

Cite this article as: Wei J, Zhang Y, Li Z, Li X, Zhao C. Docetaxel population pharmacokinetic modelling and simulation in Chinese cancer patients. Ann Transl Med 2022;10(12):705. doi: 10.21037/atm-22-2619

© Annals of Translational Medicine. All rights reserved.

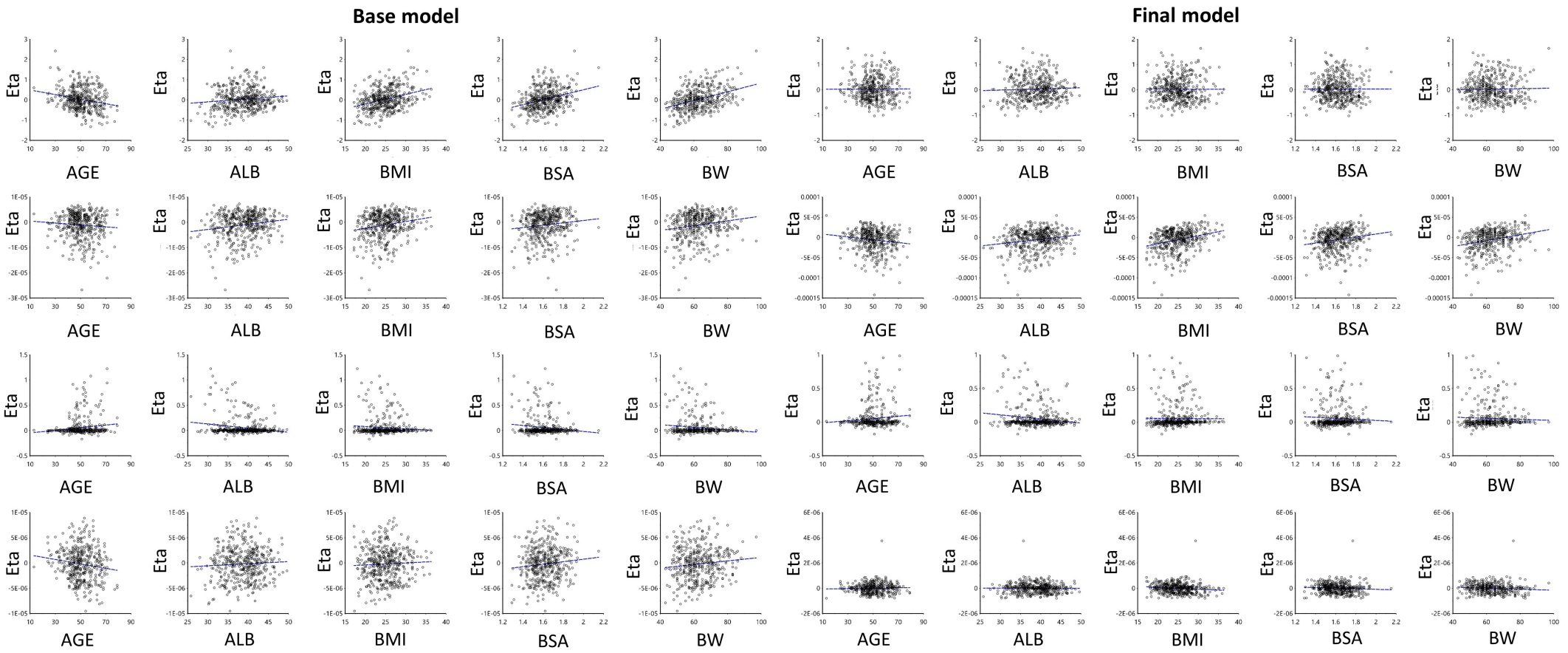

Figure S1 Plots of correlation between pharmacokinetics parameters and all covariates in the base and final models. Eta, ETAS (η); ETAS, inter-individual variations in pharmacokinetic parameters; BMI, body mass index; ALB, albumin; BSA, body surface area; BW, body weight.

© Annals of Translational Medicine. All rights reserved.
https://dx.doi.org/10.21037/atm-22-2619